

Red cell membrane and plasma linoleic acid nitration products: Synthesis, clinical identification, and quantitation

Paul R. S. Baker*, Francisco J. Schopfer*, Scott Sweeney, and Bruce A. Freeman†

Departments of Anesthesiology, Biochemistry, and Molecular Genetics and Center for Free Radical Biology, University of Alabama at Birmingham, Birmingham, AL 35294

Edited by Louis J. Ignarro, University of California School of Medicine, Los Angeles, CA, and approved June 9, 2004 (received for review April 19, 2004)

Nitric oxide (*NO) and its reactive metabolites mediate the oxidation, nitration, and nitrosation of DNA bases, amino acids, and lipids. Here, we report the structural characterization and quantitation of two allylic nitro derivatives of linoleic acid (LNO₂), present as both free and esterified species in human red cell membranes and plasma lipids. The LNO₂ isomers 10-nitro-9-*cis*,12-*cis*-octadecadienoic acid and 12-nitro-9-*cis*,12-*cis*-octadecadienoic acid were synthesized and compared with red cell and plasma LNO₂ species based on chromatographic elution and mass spectral properties. Collision-induced dissociation fragmentation patterns from synthetic LNO₂ isomers were identical to those of the two most prevalent LNO₂ positional isomers found in red cells and plasma. By using [¹³C]LNO₂ as an internal standard, red cell free and esterified LNO₂ content was 50 ± 17 and 249 ± 104 nM, respectively. The free and esterified LNO₂ content of plasma was 79 ± 35 and 550 ± 275 nM, respectively. Nitrated fatty acids, thus, represent the single largest pool of bioactive oxides of nitrogen in the vasculature, with a net LNO₂ concentration of 477 ± 128 nM, excluding buffy coat cells. These observations affirm that basal oxidative and nitrating conditions occur in healthy humans to an extent that is sufficient to induce abundant membrane and lipoprotein–fatty acid nitration. Given that LNO₂ is capable of mediating cGMP and non-cGMP-dependent signaling reactions, fatty acid nitration products are species representing the convergence of *NO and oxygenated lipid cell-signaling pathways.

Nitric oxide (*NO) is an endogenous mediator of cell function that acts predominantly by means of the stimulation of soluble guanylate cyclase (1). In addition to regulating vascular relaxation, *NO modulates oxidative and free radical reactions, inflammatory cell function, posttranslational protein modification, neurotransmission, and regulation of gene expression (2–5). *NO exerts a particularly broad influence on oxidative inflammatory reactions by reacting at diffusion-limited rates with superoxide (*O₂^{•-}, $k = 1.9 \times 10^{10} \text{ M}^{-1}\text{sec}^{-1}$) to yield peroxynitrite (ONOO⁻) and its conjugate acid, peroxynitrous acid (ONOOH), the latter of which undergoes homolytic scission to nitrogen dioxide (*NO₂) and hydroxyl radical (*OH) (2, 6). Also, biological conditions favor the reaction of ONOO⁻ with CO₂, generating nitrosoperoxycarbonate (ONO-OCO₂⁻; $k = 3 \times 10^4 \text{ M}^{-1}\text{sec}^{-1}$), which yields *NO₂ and carbonate (*CO₃⁻) radicals by means of homolysis or rearranges to NO₃⁻ and CO₂ (7). During inflammation, neutrophil myeloperoxidase and heme proteins, such as myoglobin and cytochrome *c*, form H₂O₂-dependent Compound I intermediates that are direct oxidants and catalyze the consumption of *NO and the oxidation of nitrite (NO₂⁻) to *NO₂ (8–11). Although the rate of reaction of *NO with O₂ is slow ($k = 2 \times 10^6 \text{ M}^{-2}\text{sec}^{-1}$), the small molecular radius, uncharged nature, and lipophilicity of *NO and O₂ facilitate their diffusion and concentration in membranes and lipoproteins up to 20-fold (12–14). This “molecular lens” effect that is induced by solvation in hydrophobic cell compartments accelerates the reaction of *NO with O₂ to yield N₂O₃ and N₂O₄. As a consequence of this diversity of *NO reactions with partially reduced oxygen

species, a rich spectrum of products is formed that orchestrates target molecule oxidation, nitrosation, and nitration reactions.

Multiple mechanisms account for the nitration of fatty acids by *NO-derived species (15–20). During both basal cell-signaling and tissue-inflammatory conditions, *NO₂ that is generated by the aforementioned reactions can react with membrane and lipoprotein lipids. Environmental sources also yield *NO₂ as a product of combustion. *NO₂ initiates autooxidation of polyunsaturated fatty acids by means of hydrogen abstraction from the bis-allylic carbon, to form nitrous acid and a resonance-stabilized allylic radical (21). This lipid radical species predominantly reacts with molecular oxygen to form a peroxy radical. During the unique oxidation–reduction conditions of inflammation or ischemia–reoxygenation, tissue O₂ levels are often suppressed and nitrogen oxide levels are elevated, favoring lipid radical reaction with *NO₂ to yield multiple nitration products, including nitrated nitrohydroxy and dinitro fatty acid derivatives (18, 19, 21). Polyunsaturated fatty acids can also be nitrated by acidified nitrite (HNO₂), generating a complex mixture of products that are similar to those formed by direct reaction with *NO₂, including singly nitrated species that maintain the bis-allylic bond arrangement (18, 19). Acid-catalyzed fatty acid nitration is expected during physiological and pathological conditions in which NO₂⁻ is exposed to low pH (e.g., pH < 4.0), such as in the gastric compartment after endosomal or phagolysosomal acidification or in tissues after postschemic reperfusion.

Nitrated linoleic acid (LNO₂)[‡] displays robust cell-signaling activities that appear to be antiinflammatory (20, 22–25). LNO₂ inhibits platelet function by means of cAMP-dependent mechanisms (26), and it inhibits neutrophil O₂^{•-} generation, calcium influx, elastase release, CD11b expression, and degranulation by means of non-cAMP-dependent, non-cGMP-dependent mechanisms (23). LNO₂ also induces vessel relaxation, in part by means of cGMP-dependent mechanisms (22, 27). In aggregate, these data infer that nitrated unsaturated fatty acids represent a class of lipid-derived signaling mediators. At present, a lack of clinical quantitation and structural characterization of nitrated fatty acids has limited the establishment of LNO₂ derivatives as biologically

This paper was submitted directly (Track II) to the PNAS office.

Abbreviations: EI, electron impact; EPI, enhanced product ion; ESI, electrospray ionization; MRM, multiple reaction monitor(ing); MS/MS, tandem MS; NICI, negative-ion chemical ionization; PFB, pentafluorobenzyl.

See Commentary on page 11527.

*P.R.S.B. and F.J.S. contributed equally to this work.

†To whom correspondence should be addressed at: 304/8 Biomedical Research Building II, 901 19th Street South, University of Alabama at Birmingham, Birmingham, AL 35233. E-mail: freerad@uab.edu.

[‡]Nitrated linoleic acid is termed LNO₂. Nitrohydroxy and dinitro adducts of LNO₂ are referred to as L(OH)NO₂ and L(NO₂)₂, respectively. Linoleic acid singly nitrated at either the 10 or 12 carbon, with retention of the *cis*–*cis* bis-allylic bond arrangement are referred to as C10-LNO₂ and C12-LNO₂, respectively. International Union of Pure and Applied Chemistry nomenclature defines these species as 10-nitro-9-*cis*,12-*cis*-octadecadienoic acid and 12-nitro-9-*cis*,12-*cis*-octadecadienoic acid, respectively.

© 2004 by The National Academy of Sciences of the USA

relevant lipid-signaling mediators. Here, we report that both free and esterified linoleate nitration products are abundant in healthy human red cell and plasma lipids. By using GC-MS and HPLC-MS, 10-nitro-9,12-octadecadienoic acid and 12-nitro-9-*cis*,12-*cis*-octadecadienoic acid were clinically identified and quantitated.

Experimental Procedures

Materials. Linoleic acid was obtained from Nu Check Prep (Elysian, MN). Phenylselenium bromide, mercury chloride, sodium nitrite, anhydrous tetrahydrofuran, *N,N*-diisopropylethylamine (99.5%) and acetonitrile were from Sigma-Aldrich. Silica gel HF thin-layer chromatography (TLC) plates (250 μm) were obtained from Analtch. Pentafluorobenzyl (PFB) bromide and methanolic BF_3 were obtained from Pierce. The solvents used in syntheses were HPLC grade or better (Fisher Scientific). Solvents for MS analyses were obtained from Burdick and Jackson. We obtained [^{13}C]linoleic acid from Spectra Stable Isotopes (Columbia, MD), and [^{15}N]NaNO₂ was obtained from Cambridge Isotope Laboratories (Cambridge, MA). We synthesized [^{14}N]LNO₂, [^{13}C]LNO₂, and [^{15}N]LNO₂ positional isomers, as described in the legends to Figs. 4 and 5, which are published as supporting information on the PNAS web site.

Red Blood Cell and Plasma Lipid Isolation and Extraction. Peripheral blood from healthy human volunteers was collected (with Institutional Review Board approval) by venipuncture in heparinized tubes and centrifuged (1,200 $\times g$ for 10 min), and plasma was isolated from red cell pellets from which the buffy coat was removed. Lipid extracts were then prepared from packed red cells and plasma (28) and analyzed by MS. Care was taken to avoid acidification during all steps of plasma fractionation and lipid extraction. Lipid extracts from plasma were fractionated by TLC to separate LNO₂ from the bulk of neutral lipids present in plasma, minimizing ionization dampening during LNO₂ analysis by MS. To measure the esterified LNO₂ content in red cell membranes and plasma lipoproteins, lipid extracts were first hydrolyzed (29), fractionated by TLC, and analyzed by MS.

Analysis of Synthetic LNO₂ Methyl and PFB Esters by GC-MS. Methyl esters of synthetic LNO₂ isomers were analyzed by GC-MS in both positive- and negative-ion modes. Electron-impact (EI) ionization was used to identify and characterize the fragmentation patterns of the two main positional isomers of LNO₂ methyl esters. EI GC-MS was performed by using a Saturn 2000 MS coupled with a 3800 GC (Varian). Samples were ionized by EI at +70 eV and resolved by GC using a CP-7420 capillary column (i.d., 0.25 mm; fused silica, 100 m; Varian). Helium was used as the carrier gas.

Because of the low sensitivity of positive-ion GC-MS to LNO₂, negative-ion chemical ionization (NICI) was used to characterize PFB esters of synthetic LNO₂ and detect LNO₂ species *in vivo*. PFB esters of synthetic LNO₂ were prepared, as well as red cell and plasma lipids (28), with biological lipids first partially purified by TLC. Lipids were then analyzed by NICI GC-MS by using a 5890 GC (Hewlett-Packard) coupled to a single-quadrupole MS (Hewlett-Packard) using a 30-m CP-Sil 8CB MS column (5% phenyl/95% dimethylpolysiloxane; Varian) (30).

Analysis of LNO₂ Positional Isomers by ESI Tandem MS (MS/MS). Qualitative analysis of nitrated linoleic acid positional isomers by electrospray ionization (ESI) MS was performed by using a hybrid triple-quadrupole linear ion-trap MS (Applied Biosystems/MDS Sciex, Thornhill, ON, Canada). Positional isomers of LNO₂ were resolved by reverse-phase HPLC using a 150 \times 2-mm C18 Luna column (particle size, 3 μm ; Phenomenex, Belmont, CA). Resolved isomers were detected by MS using a multiple reaction-monitoring (MRM) scan mode by reporting molecules that undergo an m/z 324/277 mass transition. This transition, consistent with the loss of HNO₂ [$\text{M}-(\text{HNO}_2)\text{-H}^-$], is common for all mononitrated isomers of linoleic acid. Concurrent with MRM, enhanced product ion

(EPI) analysis was performed to generate characteristic and identifying fragmentation patterns of the eluting species with a precursor mass of $m/z = 324$.

Detection and Quantitation of LNO₂ in Human Red Blood Cells and Plasma. Quantitation of LNO₂ was performed as described above, with the following modifications: [^{13}C]LNO₂ was added as internal standard to correct for losses during extraction and TLC, and the gradient elution profile was changed so that all LNO₂ positional isomers eluted at the same time. The following two MRM transitions were monitored: $m/z = 324/277$ (LNO₂) and $m/z = 342/295$ ([^{13}C]LNO₂). The ratio of analyte to internal standard areas was determined, and LNO₂ content was quantitated by using ANALYST 1.4 (Applied Biosystems).

Results

Synthesis of LNO₂. Modification of a nitrosenylation-mediated linoleic acid nitration reaction (Fig. 4A) increased the purity and yield of fatty acid allylic nitration products significantly, facilitating the structural resolution of specific LNO₂ positional isomers (22, 31, 32). Preparative TLC permitted the initial resolution of nitrated fatty acids from starting materials and oxidized linoleic acid species (Fig. 4B). These changes in synthetic approaches increased linoleic acid nitration product yield from 4% to >50% (22).

Spectral Analysis of LNO₂. Nitrated linoleic acid displays a characteristic absorption profile and maximum, providing determination of an extinction coefficient and a method for measuring concentrations of synthetic LNO₂. This species displays a unique absorbance maximum at 329 nm, compared with linoleic acid (Fig. 5A). Plotting absorbance versus concentration profiles for each of the synthetic LNO₂ preparations reported here, [^{14}N]LNO₂, [^{15}N]LNO₂, and [^{13}C]LNO₂, generated identical extinction coefficients for all LNO₂ derivatives: $\epsilon = 10.1 \text{ cm}^{-1}\text{M}^{-1}$ (Fig. 5B).

GC-MS Analysis of LNO₂. EI GC-MS of LNO₂ methyl esters revealed two dominant peaks at 38.75 and 39 min, when resolved by using a 100-m column (Fig. 1A). Product ion analysis of each peak (Fig. 1C) generated fragmentation patterns that were similar to NMR-verified patterns reported (18) for acidic nitration of ethyl linoleate. The first and second peaks correspond to linoleic acid that is nitrated on the C12 and C10, respectively. These two isomers are identified by the unique daughter ions $m/z = 250$ and $m/z = 282$ (specific to C12), and $m/z = 196$ (specific to C10). Analysis of [^{15}N]LNO₂ revealed fragmentation patterns with these identifying ions shifted by $m/z = +1$, further affirming fragments containing the nitro group (Fig. 1C).

Although it is useful for structural analysis of synthetic LNO₂ isomers, EI GC MS lacks sensitivity for the detection of LNO₂ derivatives present in biological samples. Thus, these analyses were performed by NICI GC-MS on PFB derivatives of LNO₂ (Fig. 1B). Chromatographic separation of both synthetic LNO₂ and TLC-separated red cell lipid extracts resolved two dominant peaks, C12 and C10, and two minor peaks ascribed to either *cis-trans* or C13 and C9 positional isomers of LNO₂. In both cases, >90% of total peak area is accounted for by the C12 and C10 isomers. The C12 and C10 positional isomers of LNO₂-PFB derivatives were confirmed to be the same as those identified as LNO₂ methyl esters by EI GC-MS (data not shown). Initial detection and quantitation of endogenous levels of LNO₂ was performed by using NICI GC-MS; however, extensive sample processing and limited sensitivity motivated an HPLC-MS/MS-based method to characterize and quantitate LNO₂ in biological samples.

Synthetic and Endogenous LNO₂ Isomer Characterization by ESI MS/MS. An HPLC separation strategy that baseline-resolved individual LNO₂ isomers permitted the liquid chromatography/MS-based characterization of LNO₂ derivatives in biological samples (Fig.

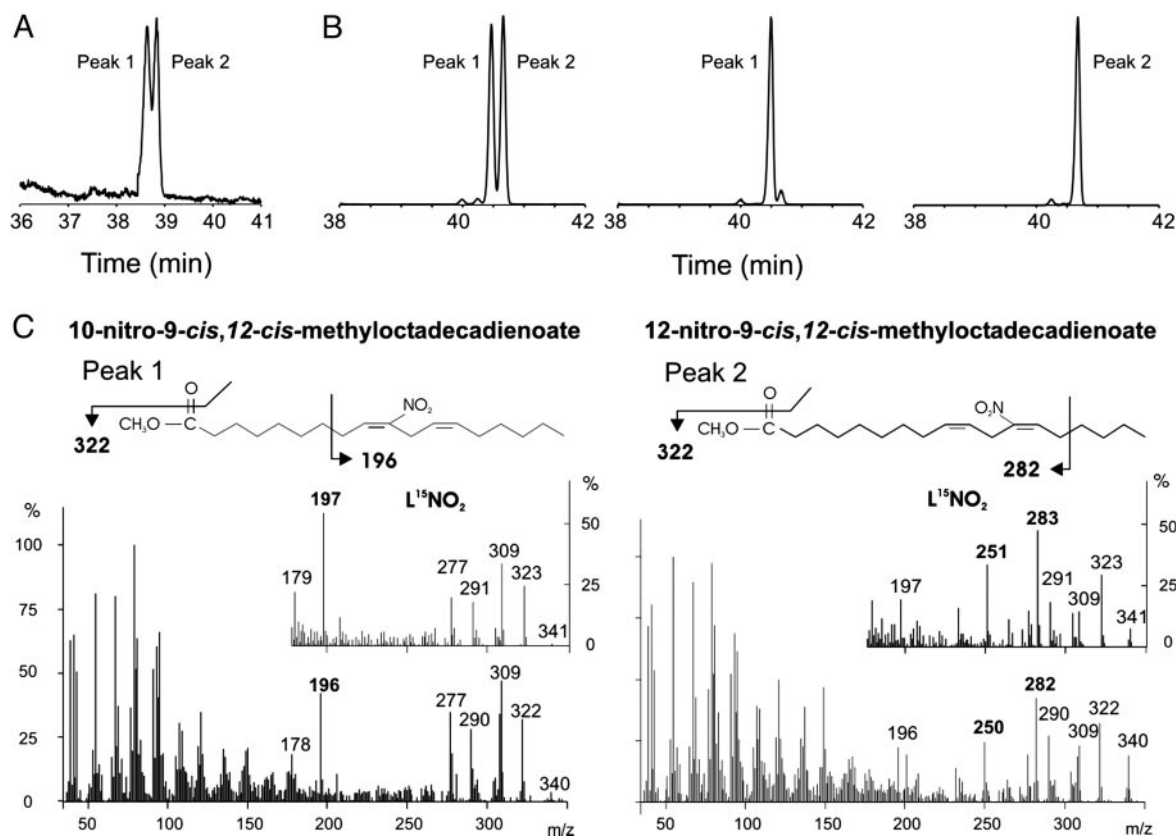


Fig. 1. Characterization of LNO₂ by GC-MS. (A) LNO₂ methyl esters were resolved by using a 100-m fused silica column and detected by total ion-count monitoring after EI ionization. Peak 1 (38.75 min) corresponds to linoleic acid nitrated at the 12-carbon (C12), and Peak 2 (39.00 min) corresponds to nitration on the 10-carbon (C10). (B) LNO₂ and HPLC-separated positional isomers of LNO₂ were derivatized to their PFB esters, resolved on a 30-m CP-Sil 8CB MS, and detected by using NICI GC-MS. Peaks 1 and 2 correspond to C12 and C10 isomers, respectively. These species account for 90–95% of the total peak areas. (C) EI spectra were obtained from the peaks shown in A. Unique fragments (namely, $m/z = 196$ for C10, and $m/z = 250$ and $m/z = 282$ for C12) were detected that enabled structural identification of the isomers.

2A). To initially identify individual LNO₂ isomers resolved by HPLC separation, the two major species were collected (peaks 1 and 2, Fig. 2A), derivatized to PFB esters, and analyzed by GC-MS. From GC-MS analysis, the first species eluting upon HPLC separation was identified as the C12 isomer, and the second species was identified as the C10 nitro derivative (Fig. 1B). The linear ion-trap mode of the hybrid MS was used to perform EPI analysis on eluting peaks to generate an identifying fragmentation pattern for each LNO₂ positional isomer (Fig. 2B, graph 1, and C, graph 1). MS/MS analysis of C10 LNO₂ revealed unique fragments, $m/z = 168$ and $m/z = 228$, as well as fragments common to all LNO₂ isomers ($m/z = 233, 244, 277, 293,$ and 306 ; Fig. 2C, graph 1). The $m/z = 228$ ion was further fragmented in the ion trap by using the MS³ scanning mode, generating a fragment with $m/z = 46$, indicating the loss of an allylic nitro group and assigning the nitro group to the C9 double bond. MS/MS analysis of C12-LNO₂ generated unique fragments ($m/z = 196$ and $m/z = 157$) and the common fragments listed above (Fig. 2B, graph 1). In aggregate, from the synthetic rationale and GC-MS and ESI MS/MS data, the C10 and the C12 isomers are identified as 10-nitro-9-*cis*,12-*cis*-octadecadienoic acid and 12-nitro-9-*cis*,12-*cis*-octadecadienoic acid, respectively.

ESI MS/MS was used to characterize and quantitate LNO₂ species present in human red cells and plasma (Fig. 2). The MRM elution profiles for red cell and plasma lipid extracts were identical to those obtained for synthetic standards (Figs. 2B, graphs 2 and 3, and C, graphs 2 and 3). All characteristic fragments found in the EPI spectra of the synthetic C10 and C12 LNO₂ isomers were present in the resolved biological extracts, affirming that red cells

and plasma contain LNO₂ positional isomers with chromatographic profiles and fragmentation patterns that are identical to our synthetic standards. It is possible that the configuration of the double bond in endogenous LNO₂ may differ from synthetic standards (i.e., the *cis-cis* configuration may be *cis-trans* or *trans-cis*), with a level of structural detail not being provided by EPI analysis.

Quantitation of Free and Esterified LNO₂ in Red Blood Cells and Plasma. To quantitate net LNO₂ species present in red cells and plasma, HPLC gradient conditions were changed so that all positional isomers coeluted (Fig. 3A). Nitrated linoleic acid concentrations were calculated as a function of the ratio of analyte to internal standard peak areas by using an internal standard curve linear over five orders of magnitude (Fig. 3B). Blood samples obtained from 10 healthy human volunteers (five female and five male, ranging 22–45 years of age) revealed free LNO₂ in red cells (i.e., LNO₂ not esterified to glycerophospholipids or neutral lipids) to be 50 ± 17 pmol/ml packed cells. Total free and esterified LNO₂, the amount present in saponified samples, was 249 ± 104 pmol/ml packed cells. Thus, $\approx 75\%$ of LNO₂ in red cells exists in the esterified form. In plasma, free and total (free plus esterified) LNO₂ was 79 ± 35 and 630 ± 240 nM, respectively, with free LNO₂ representing 85% of total (Table 1) (33–37).

Discussion

Cell-signaling studies have revealed that synthetic LNO₂ manifests bioactivities that are generally antiinflammatory. Allylic nitro derivatives of linoleic acid inhibit neutrophil degranulation, $^{\circ}\text{O}_2^-$

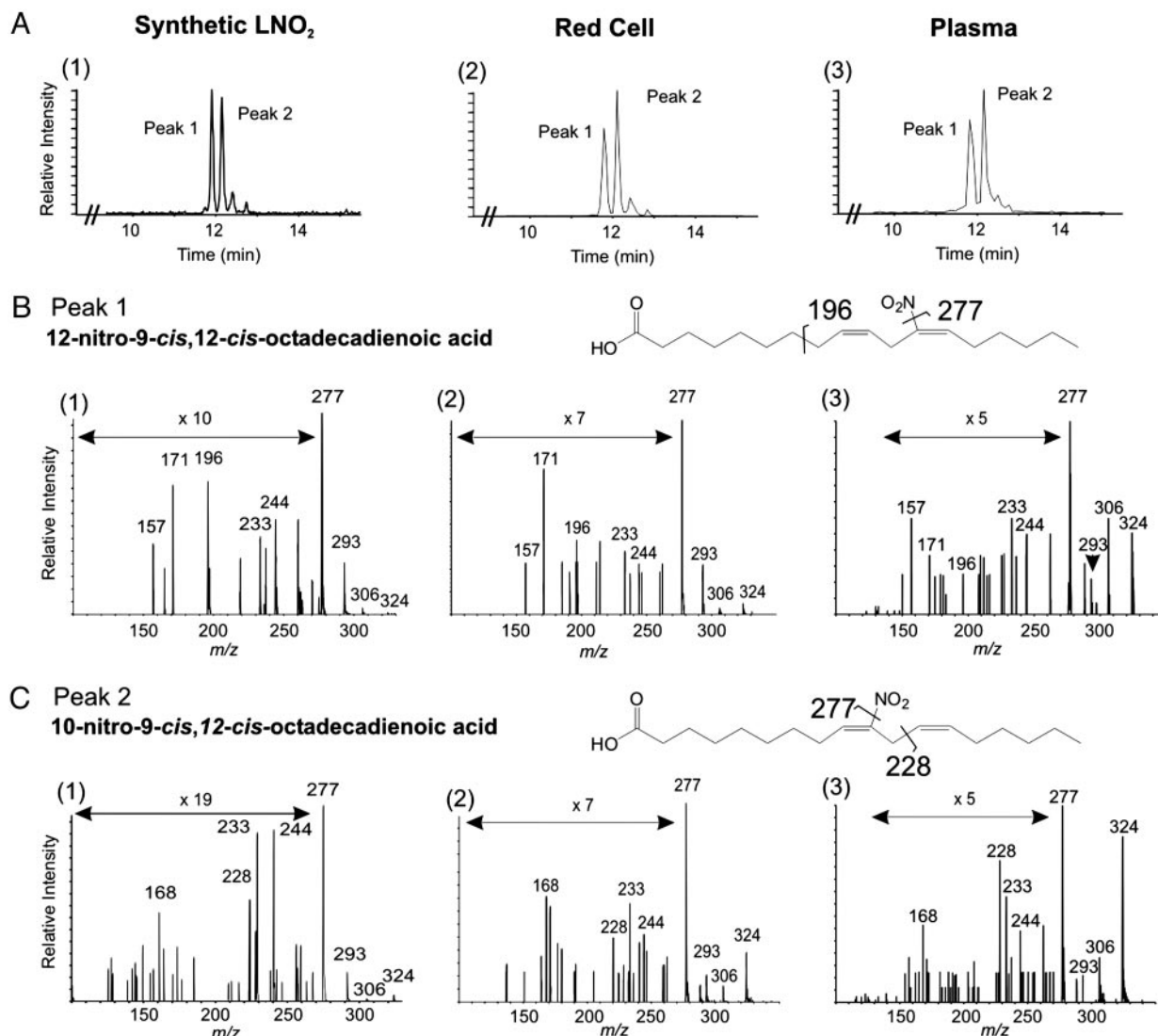


Fig. 2. Characterization of LNO₂ by ESI triple-quadrupole MS. (A) Synthetic LNO₂ positional isomers were separated by HPLC and detected by MS/MS in the MRM mode by monitoring the 324/277 collision-induced dissociation transition (graph 1). No other peaks were detected in the chromatogram. The same method was used to resolve LNO₂ isomers present in the total lipid extract from 1 ml of packed red blood cells (graph 2) and plasma (graph 3). (B) EPI analysis of Peak 1, revealing fragments unique to the C12 positional isomer of LNO₂, $m/z = 196$ and $m/z = 157$, plus fragments common to all LNO₂ isomers ($m/z = 233, 244, 277, 293$, and 306) (graph 1). EPI analyses of Peak 1 for red cell (graph 2) and plasma (graph 3) lipid extracts gave similar fragmentation patterns. All identifying fragments from graph 1 are present in graphs 2 and 3. (C). In addition to the common fragment ions of LNO₂, peak 2 displayed unique fragments $m/z = 228$ and $m/z = 168$ (graph 1). These fragments, particularly $m/z = 228$, indicate nitration of the C10 of LNO₂. EPI spectra from Peak 2 of resolved red cell (graph 2) and plasma (graph 3) lipid extracts gave fragmentation patterns similar to the synthetic standard.

formation, CD11b expression, and fMLP-induced Ca²⁺ influx by means of non-cGMP-dependent, protein kinase-mediated actions (23). In platelets, thrombin-induced aggregation is inhibited upon LNO₂-mediated attenuation of cAMP-dependent Ca²⁺ mobilization and activation of the phosphorylation of vasodilator-stimulated phosphoprotein (VASP) at Ser-157. Current evidence (26) reveals a dual regulation of platelet adenylyl cyclase and phosphodiesterase E activities by LNO₂. Additionally, LNO₂ has been shown to induce endothelium-independent, cGMP-mediated smooth muscle relaxation (22). These observations reveal that nitrated fatty acids may serve as endogenous cell-signaling molecules, a precept remaining contingent upon the identification of more discrete cell-signaling responses and the clinical detection of these species. The latter issue has been resolved by structurally characterizing linoleic acid nitration products generated by nitrosenylation and those present in human red cell and plasma lipids. By using a ¹³C-labeled internal

standard added during lipid extractions, both free and esterified LNO₂ levels were shown to be abundant in the vasculature. Here, we report that the LNO₂ positional isomers 10-nitro-9,12-octadecadienoic acid (C10) and 12-nitro-9-cis,12-cis-octadecadienoic acid (C12) are present as free acids in healthy human blood and as esterified components of red cell membranes and plasma lipoproteins, with a net concentration of ≈500 nM (Table 1). Thus, LNO₂ derivatives represent the single largest pool of bioactive oxides of nitrogen in the vascular compartment (33–37). Most of this LNO₂ is esterified (≈80%), suggesting that lipases and/or phospholipases will be central for the regulated release of nitrated free fatty acids.

Recently, nitration products of arachidonic acid (27), linoleic acid (38) and cholesteryl linoleate (39) have been reported in biological samples. Importantly, all of these observations were made after lipid extraction of nitrite-containing specimens under

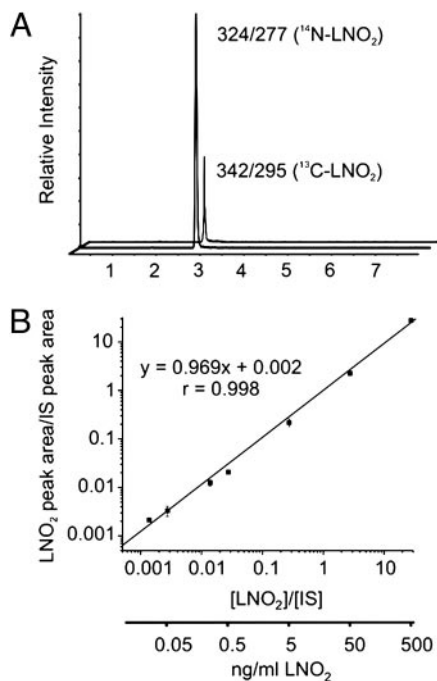


Fig. 3. Quantitative analysis of red blood cell and plasma LNO₂. (A) We added [¹³C]LNO₂ to lipid extractions as an internal standard to quantitate the free and esterified LNO₂ content of red cells and plasma obtained from healthy human volunteers. The mean age of the five female and five male subjects was 34 years. The endogenous LNO₂ isomers coeluted with the added ¹³C-labeled LNO₂ internal standard, with the internal standard differentiated from endogenous LNO₂ by monitoring its unique *m/z* = 342/295 MRM transition. (B) The internal standard curve for LNO₂ reveals linear detector responses over five orders of magnitude. The limit of quantitation (LOQ) for LNO₂, as defined by 10 times the SD of the noise, is ≈0.3 fmol (≈100 fg) injected on column.

acidic conditions (pH <4), documented to result in HNO₂-dependent fatty acid nitration and oxidation (20). This analytical pitfall raises the question of whether the various reported LNO₂

species were indeed endogenous, and it impairs an ability to determine concentration and structural characteristics. For this reason, this article includes analysis of potential confounding factors and artifacts in the detection and quantitation of linoleic acid nitration products in clinical specimens and reveals that both acid-catalyzed reactions during lipid processing and the presence of adventitious NO₂⁻ induces artifact in LNO₂ analysis. Extensive control studies ensured that the LNO₂ detected was not a byproduct of lipid extraction, storage, HPLC separation, MS analysis, or the presence of alkyl hydroxy and hydroperoxy derivatives. We added [¹³C]linoleic acid as a reporter molecule before red cell and plasma lipid purification and analysis during methods development, which permitted the MS detection of any possible ¹³C-labeled LNO₂ products being formed. Also, up to 200 μM NO₂⁻ was included in initial lipid extractions to determine whether separations or analysis-induced nitration reactions might be supported by physiological NO₂⁻ levels that can exceed 200 nM (34, 35). All critical phases of lipid extraction avoided the use of acidic pH to limit acid-catalyzed, HNO₂-dependent lipid nitration reactions. Moreover, the addition and recovery of an LNO₂ internal standard to biological lipid extractions showed efficient extraction of lipids of interest at neutral pH. Together, control studies affirmed that in this study, no LNO₂ derivatives were generated during the *ex vivo* processing of clinical samples and subsequent lipid purification and analysis steps.

Nitrated lipids can be synthesized *ex vivo* by different approaches, with varying degrees of specificity and yield. Acid-catalyzed, HNO₂-dependent fatty acid nitration readily nitrates lipids; however, multiple species, including conjugated dienes, nitro, hydroxy, hydroperoxy, nitrohydroxy, and nitrohydroperoxy adducts are formed, with all products displaying nonspecific stereochemistry (18). This reaction pathway may also occur in select biological milieu, such as the low pH environment of the gastric system and upon endosome acidification (40). Linoleic acid nitration by nitrosylation generates primarily two derivatives of linoleic acid (C10 and C12 LNO₂) with no rearrangement of the olefinic groups (41), thus simplifying structural characterization and fortuitously yielding positional isomers that are identical to those of red cell and lipoprotein lipids.

The characterization of synthetic LNO₂ species was performed by both GC-MS and HPLC-MS. Analysis of synthetic LNO₂ methyl ester products by EI GC-MS indicated that linoleic acid was singly

Table 1. Biologically active nitrogen oxide derivatives in human blood: Comparison with nitrated linoleic acid

Species	Compartment	Fraction	Concentration, nM	Source
NO ₂ ⁻	Plasma	Total	205 ± 21	35, 36
RSNO	Plasma	Total	7.2 ± 1.1	35, 36
3-Nitro-tyrosine	Plasma	Total	0.74 ± 0.30	38
LNO ₂	Plasma	Free	79 ± 35	—
		Esterified	550 ± 275	This article
		Total	630 ± 240	
Hb-NO	Blood	Total	<50	37
Hb-SNO	Blood	Total	0–150	34
LNO ₂	Packed red cells	Free	50 ± 17	—
		Esterified	199 ± 121	This article
		Total	249 ± 104	
LNO ₂	Whole blood*	Total	477 ± 128*	This article

Venous blood was obtained from healthy human volunteers and centrifuged (1,200 × *g* for 10 min), and plasma was isolated from red cell pellets from which the buffy coat was removed. Total lipid extracts were prepared from packed red cells and plasma (28) and analyzed by MS, as described in *Experimental Procedures*. Total LNO₂ (free plus esterified) was determined in lipid extracts after saponification. Free and total LNO₂ was quantitated by fitting analyte to internal standard area ratios obtained by MS to an internal standard curve. Concentration values for other bioactive oxides of nitrogen were obtained from the literature. It is noted that nitrite is readily oxidized to nitrate, making precise quantitation of nitrite problematic. Data are expressed as mean ± SD (*n* = 10; 5 female and 5 male). RSNO S-nitrosothiols; Hb-NO, heme nitrosyl; Hb-SNO, S-nitrosohemoglobin.

*Assuming a 40% hematocrit.

nitration and not oxidized, with the purified product mixture containing two major nitration products (Fig. 1). Unlike CID fragmentation patterns, which depend on numerous instrument and analysis characteristics, EI fragmentation patterns for a particular molecule remain consistent. Thus, we compared the EI fragmentation patterns of nitrosylation-induced linoleate nitration products with NMR-verified fragmentation patterns of methyl esters of linoleic acid nitrated by exposure to HNO₂ (18). The EI fragmentation patterns of peak 1 and peak 2 upon GC separation were identical to those generated from LNO₂ nitrated at the C12 and C10, respectively. Although EI GC-MS provided essential structural information about synthetic LNO₂, this technique has limited sensitivity for anionic fatty acids, especially when present in complex biological lipid mixtures. Analysis of PFB esters of LNO₂ by NICI GC-MS provided a degree of sensitivity that allowed *in vivo* detection of LNO₂ (data not shown); however, this approach requires extensive sample preparation and has limited quantitative precision. Thus, ESI MS/MS was used to characterize and quantify synthetic and endogenous LNO₂. Unique HPLC retention times and fragmentation patterns for each synthetic LNO₂ isomer were obtained by CID, which provided a “molecular fingerprint” that was used to identify LNO₂ isomers in biological samples (Fig. 2). These fragmentation patterns were obtained by using an ion-trap mode (EPI) of a hybrid MS, providing enhanced sensitivity to minor fragments and more detailed structural information. The *m/z* = 228 fragment generated from the second eluting peak, barely detectable without trapping, permitted the assignment of the NO₂ functional group to the C9 double bond.

In summary, two positional isomers of LNO₂ have been synthesized, resolved, and structurally characterized, with corresponding species identified and quantitated in human blood. Allylic nitro derivatives of fatty acids display unique vascular and inflammatory cell-signaling activities and appear to represent a novel class of lipid-signaling molecules. Whereas NO-dependent oxidation and nitration reactions will induce nitration of endogenous tissue fatty acids, dietary NO₂⁻ or nitrated lipids may also contribute to tissue LNO₂ content. *In vitro* studies presently support the precept that allylic nitro derivatives of fatty acids counter the proinflammatory signaling actions of most eicosanoids, thus these byproducts of inflammatory oxidation and nitration reactions will contribute to the resolution of inflammation. In aggregate, these observations reveal that allylic nitro derivatives of unsaturated fatty acids represent the convergence of NO and oxidized lipid cell-signaling pathways. Indeed, LNO₂ undergoes high-affinity receptor–ligand interactions (F.J.S., Y. Lin, P.R.S.B., Y. E. Chen, and B.A.F., unpublished data) that induce alterations in gene expression and the induction or suppression of multiple cell growth control and inflammatory-related proteins.

We thank Drs. Sai Chang, Tom Bisenthal, and Nadia Pace (Applied Biosystems/MDS Sciex); Dr. Bruce King (Wake Forest University, Winston-Salem, NC); and Drs. Bill Cauffman and Greg Gorman (Southern Research Institute, Birmingham, AL) for their helpful input. This work was supported by National Institutes of Health Grants RO1HL58115 and RO1HL64937. P.R.S.B. was supported by National Institutes of Health Cardiovascular Hypertension Training Grant T32HL07457.

- Arnold, W. P., Mittal, C. K., Katsuki, S. & Murad, F. (1977) *Proc. Natl. Acad. Sci. USA* **74**, 3203–3207.
- Beckman, J. S., Beckman, T. W., Chen, J., Marshall, P. A. & Freeman, B. A. (1990) *Proc. Natl. Acad. Sci. USA* **87**, 1620–1624.
- Nathan, C. (1992) *FASEB J.* **6**, 3051–3064.
- Jourd'heuil, D., Miranda, K. M., Kim, S. M., Espey, M. G., Vodovotz, Y., Laroux, S., Mai, C. T., Miles, A. M., Grisham, M. B. & Wink, D. A. (1999) *Arch. Biochem. Biophys.* **365**, 92–100.
- Rubbo, H., Darley-Usmar, V. & Freeman, B. A. (1996) *Chem. Res. Toxicol.* **9**, 809–820.
- Kissner, R., Nauser, T., Bugnon, P., Lye, P. G. & Koppenol, W. H. (1997) *Chem. Res. Toxicol.* **10**, 1285–1292.
- Radi, R., Denicola, A. & Freeman, B. A. (1999) *Methods Enzymol.* **301**, 353–367.
- Baldus, S., Eiserich, J. P., Mani, A., Castro, L., Figueroa, M., Chumley, P., Ma, W., Tousson, A., White, C. R., Bullard, D. C., *et al.* (2001) *J. Clin. Invest.* **108**, 1759–1770.
- Castro, L., Eiserich, J. P., Sweeney, S., Radi, R. & Freeman, B. A. (2004) *Arch. Biochem. Biophys.* **421**, 99–107.
- Eiserich, J. P., Baldus, S., Brennan, M. L., Ma, W., Zhang, C., Tousson, A., Castro, L., Lusa, A. J., Nauseef, W. M., White, C. R., *et al.* (2002) *Science* **296**, 2391–2394.
- Grisham, M. B. (1985) *J. Free Radical Biol. Med.* **1**, 227–232.
- Liu, X., Miller, M. J., Joshi, M. S., Thomas, D. D. & Lancaster, J. R., Jr. (1998) *Proc. Natl. Acad. Sci. USA* **95**, 2175–2179.
- Subczynski, W. K., Lomnicka, M. & Hyde, J. S. (1996) *Free Radical Res.* **24**, 343–349.
- Thomas, D. D., Liu, X., Kantrow, S. P. & Lancaster, J. R., Jr. (2001) *Proc. Natl. Acad. Sci. USA* **98**, 355–360.
- Rubbo, H., Radi, R., Trujillo, M., Telleri, R., Kalyanaram, B., Barnes, S., Kirk, M. & Freeman, B. A. (1994) *J. Biol. Chem.* **265**, 26066–26075.
- Gallon, A. A. & Pryor, W. A. (1993) *Lipids* **28**, 125–133.
- Gallon, A. A. & Pryor, W. A. (1994) *Lipids* **29**, 171–176.
- Napolitano, A., Camera, E., Picardo, M. & d'Ischia, M. (2000) *J. Org. Chem.* **65**, 4853–4860.
- Napolitano, A., Crescenzi, O., Camera, E., Giudicianni, I., Picardo, M. & d'Ischia, M. (2004) *Tetrahedron* **58**, 5061–5067.
- O'Donnell, V. B., Eiserich, J. P., Chumley, P. H., Jablonsky, M. J., Krishna, N. R., Kirk, M., Barnes, S., Darley-Usmar, V. M. & Freeman, B. A. (1999) *Chem. Res. Toxicol.* **12**, 83–92.
- Pryor, W. A., Lightsey, J. W. & Church, D. F. (1982) *J. Am. Chem. Soc.* **104**, 6685–6692.
- Lim, D. G., Sweeney, S., Bloodworth, A., White, C. R., Chumley, P. H., Krishna, N. R., Schopfer, F., O'Donnell, V. B., Eiserich, J. P. & Freeman, B. A. (2002) *Proc. Natl. Acad. Sci. USA* **99**, 15941–15946.
- Coles, B., Bloodworth, A., Clark, S. R., Lewis, M. J., Cross, A. R., Freeman, B. A. & O'Donnell, V. B. (2002) *Circ. Res.* **91**, 375–381.
- O'Donnell, V. B. & Freeman, B. A. (2001) *Circ. Res.* **88**, 12–21.
- O'Donnell, V. B., Chumley, P. H., Hogg, N., Bloodworth, A., Darley-Usmar, V. M. & Freeman, B. A. (1997) *Biochemistry* **36**, 15216–15223.
- Coles, B., Bloodworth, A., Eiserich, J. P., Coffey, M. J., McLoughlin, R. M., Giddings, J. C., Lewis, M. J., Haslam, R. J., Freeman, B. A. & O'Donnell, V. B. (2002) *J. Biol. Chem.* **277**, 5832–5840.
- Balazy, M., Iesaki, T., Park, J. L., Jiang, H., Kaminski, P. M. & Wolin, M. S. (2001) *J. Pharmacol. Exp. Ther.* **299**, 611–619.
- Bligh, E. G. & Dyer, W. L. (1959) *Can. J. Biochem. Physiol.* **37**, 911–917.
- Nakamura, T., Bratton, D. L. & Murphy, R. C. (1997) *J. Mass Spectrom.* **32**, 888–896.
- Wheelen, P., Zirrolli, J. A. & Murphy, R. C. (1994) *J. Am. Soc. Mass Spectrom.* **6**, 40–51.
- d'Ischia, M., Rega, N. & Barone, V. (1999) *Tetrahedron* **55**, 9297–9308.
- Ranu, B. C. & Chakraborty, R. (1991) *Tetrahedron Lett.* **32**, 3579–3582.
- Gladwin, M. T., Shelhamer, J. H., Schechter, A. N., Pease-Fye, M. E., Waclawiw, M. A., Panza, J. A., Ognibene, F. P. & Cannon, R. O., III. (2000) *Proc. Natl. Acad. Sci. USA* **97**, 11482–11487.
- Rassaf, T., Bryan, N. S., Kelm, M. & Feilisch, M. (2002) *Free Radical Biol. Med.* **33**, 1590–1596.
- Rassaf, T., Bryan, N. S., Maloney, R. E., Specian, V., Kelm, M., Kalyanaram, B., Rodriguez, J. & Feilisch, M. (2003) *Nat. Med.* **9**, 481–482.
- Cosby, K., Partovi, K. S., Crawford, J. H., Patel, R. P., Reiter, C. D., Martyr, S., Yang, B. K., Waclawiw, M. A., Zalos, G., Xu, X., *et al.* (2003) *Nat. Med.* **9**, 1498–1505.
- Soderling, A. S., Ryberg, H., Gabrielson, A., Larstad, M., Toren, K., Niari, S. & Caidahl, K. (2003) *J. Mass Spectrom.* **38**, 1187–1196.
- Lima, E. S., Di Mascio, P., Rubbo, H. & Abdalla, D. S. (2002) *Biochemistry* **41**, 10717–10722.
- Lima, E. S., Di Mascio, P. & Abdalla, D. S. (2003) *J. Lipid Res.* **44**, 1660–1666.
- Knowles, M. E., McWeeny, D. J., Couchman, L. & Thorogood, M. (1974) *Nature* **247**, 288–289.
- Hayama, T., Tomoda, S., Takeuchi, Y. & Nomura, Y. (1982) *Tetrahedron Lett.* **23**, 4733–4734.